Wind Measurements of Martian Dust Devils from HiRISE

D. S. Choi (1) and C. M. Dundas (2)

(1) Department of Planetary Sciences, University of Arizona, Tucson, AZ, USA (dchoi@lpl.arizona.edu) (2) United States Geological Survey, Flagstaff, AZ, USA

Abstract

We report direct measurements of the winds within Martian dust devils from HiRISE imagery. The central color swath of the HiRISE instrument observes the surface by using separate CCDs and color filters in rapid cadence. Active features, such as a dust devil, appear in motion when serendipitously captured by this region of the instrument. Our measurements reveal clear circulation within the vortices, and that the majority of overall wind magnitude within a dust devil is between 10 and 30 m s^{-1}.

1. Introduction

Direct measurements of the winds within a Martian dust devil [1] are challenging to obtain. Some knowledge of Martian dust devil winds stems from examination of data from meteorological instrumentation on the *Viking* landers [2], though this analysis assumes a velocity profile for the dust devil *a priori*. Other imaging studies have reported measurements of dust devil winds from both rover-based [3, 4, 5] and spacecraft [6] observations. However, these previous studies typically report the *translational* speed at which a dust devil travels across the Martian surface. The *tangential* winds within a dust devil have not been directly measured from orbital imagery except for a single measurement of the winds from *Viking* images [7]. Our approach enables direct measurements of winds within a Martian dust devil using images taken with the HiRISE (High Resolution Imaging Science Experiment) [8] camera on board the *Mars Reconnaissance Orbiter* (MRO) spacecraft.

2. Method

The central color swath of HiRISE [8] consists of separate CCDs that image the surface through independent blue-green, red, and near-IR filters. Observations with the CCDs are not simultaneous but instead separated by a short (~0.1 s) time interval. When an observation crosses an active feature such as a dust devil, changes in the active feature are apparent from the three separate views. Treating the dust clouds as passive tracers of motion then allows for the direct measurement of wind velocities.

We utilize measurements from manual (hand-eye) tracking of the clouds through image blinking, as well as automated correlation methods [9]. Typically, manual measurements are more successful than automated measurements. The relatively diffuse dust clouds, combined with the static background terrain, cause the automated software to incorrectly report the movement as stationary. Successful automated results were obtained from images with more substantial dust clouds and relatively featureless background terrain.

3. Results

Figure 1 shows wind vectors overlain on a dust devil examined for this project. Because an overall HiRISE observation is very short, we cannot track the dust devil over a discrete time to measure its translational velocity across the surface. Instead, we estimate this by calculating the overall average wind vector from the measurements, though the non-uniform spatial distribution of vectors imparts some uncertainty. The majority of overall wind measurements are between 10 and 30 m s^{-1}, though a significant portion of this measurement is the translational component. These are higher than previously reported traverse speeds (5–15 m s^{-1}, [5, 6]), though translational speeds betwen 20 and 30 m s^{-1} are not unprecedented. Typical tangential winds are lower, near 10 m s^{-1}.

Figure 2 is a radial profile of the residual winds measured using automated software within the dust devil shown in Figure 1. (The density of manual measurements is insufficient for a meaningful radial profile.) The central portion of the dust devil exhibits solid body rotation, with velocity increasing linearly with distance away from the circulation center. However, velocity at the outer region decreases with r$^{-1/2}$ away from the core, rather than the r^{-1} of a Rankine vortex.

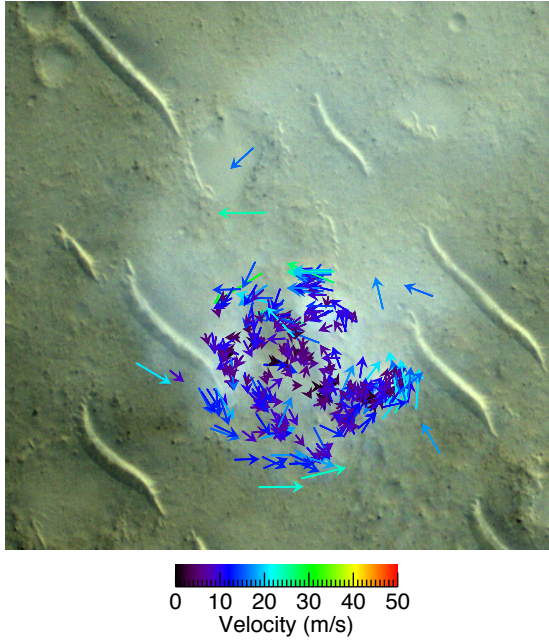ESP_013199_1900

0 10 20 30 40 50
Velocity (m/s)

Figure 1: Manually-measured, residual (i.e., corrected for estimated translational motion) wind vectors overlain on a dust devil in our data set.

This shallow decline has been observed in *in-situ* measurements of terrestrial dust devils [10] and is likely caused by surface frictional effects that break angular momentum conservation. An important caveat is that this profile is a single profile; other profiles only confirm solid body rotation in the interior, as information outside the core is either too noisy or not present.

4. Discussion

Dust devils on Mars can be kilometers in height [1]; theoretically, this induces parallax motion in the image dust clouds because of spacecraft motion between individual images. As determined from shadow lengths, all dust devils in our study are less than 1 km in height, greatly diminishing the parallax effect. In addition, non-map projected images simplify the parallax correction because the vertical axis of these images is parallel to the spacecraft ground track.

Furthermore, HiRISE applies a time-delay integration (TDI) technique to improve signal-to-noise, but the TDI time for CCDs with different filters is not necessarily the same within an image. This effectively introduces some smearing of features due to dust devil movement during TDI, but this time is always an order
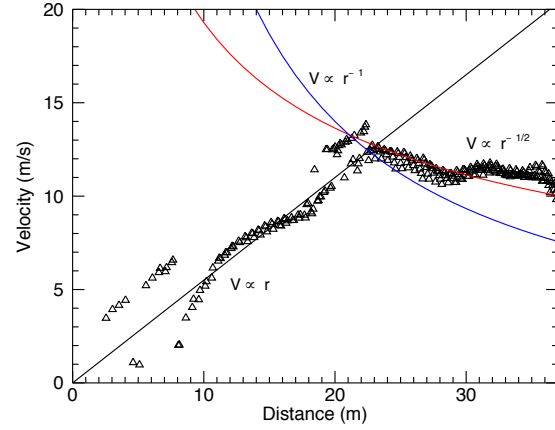

Figure 2: A radial profile from the dust devil in ESP_013199_1900 exhibiting a $r^{-1/2}$ dependance in the residual vectors, instead of a r^{-1} dropoff assumed in a Rankine profile.

of magnitude less than the image interval, mitigating this particular effect.

References

[1] Balme, M. et al. (2006) *Reviews of Geophysics*, *44*: 3003.

[2] Ringrose, T. J., et al. (2003) *Icarus*, *163*: 78–87.

[3] Metzger, S. M., et al. (1999) *Geophysical Review Letters*, *26*: 2781–2784.

[4] Greeley, R., et al. (2006) *JGR-Planets*, *111*: E12S09.

[5] Greeley, R., et al. (2010) *Journal of Geophysical Research (Planets)*, *115*: E00F02.

[6] Stanzel, C., et al. (2008) *Icarus*, *197*: 39–51.

[7] Cantor, B. A., et al. (2006) *JGR-Planets*, *111*: E12002.

[8] McEwen, A. S., et al. (2007) *JGR-Planets*, *112*: E05S02.

[9] Choi, D. S., et al. (2007) *Icarus*, *188*: 35–46.

[10] Tratt, D. M., et al. (2003) *Journal of Geophysical Research (Planets)*, *108*: 5116.